Neuroscience 142 (2006) 739–752

ECTOPIC EXPRESSION OF DOUBLECORTIN PROTECTS ADULT RAT PROGENITOR CELLS AND HUMAN GLIOMA CELLS FROM SEVERE OXYGEN AND GLUCOSE DEPRIVATION

M. SANTRA,[a] X. SHUANG LIU,[a] S. SANTRA,[a] J. ZHANG,[a] R. LAN ZHANG,[a] Z. GANG ZHANG[a] AND M. CHOPP[a,b]*

[a]*Department of Neurology, Henry Ford Health Sciences Center, Detroit, MI 48202, USA*

[b]*Department of Physics, Oakland University, Rochester, MI 48309, USA*

Abstract—Doublecortin (DCX) is a microtubule-associated protein expressed in migrating neuroblasts. DCX expression is increased in subventricular zone (SVZ) cells migrating to the boundary of an ischemic lesion after induction of middle cerebral artery occlusion (MCAO) in adult rats and mice. We tested the hypothesis that DCX, in addition to being a marker of migrating neuroblasts, serves to protect neuroblasts from conditions of stress, such as oxygen and glucose deprivation (OGD). Using gene transfer technology, we overexpressed DCX in rat SVZ and U-87 human glioma cells. The cells remained viable against severe OGD, up to 32 h exhibiting 1% apoptosis compared with 100% apoptosis in control. In addition, these genetically modified cells upregulated expression of E-, VE- and N-cadherin, molecules that promote endothelial survival signals via the VE-cadherin/vascular endothelial growth factor receptor–2/phosphoinositide 3-kinase (PI3-K)/AKT/β-catenin pathway and inactivate the proapoptotic factor Bad. DCX overexpression also significantly increased cell migration in SVZ tissue explants and U-87 cells and significantly upregulated microtubule-associated protein-2 (MAP2) and nestin protein levels in SVZ and U-87 cells compared with wild-type control cells. Knocking down DCX expression in DCX overexpressing SVZ and U-87 cells with DCX small interfering RNA (siRNA), confirmed the specificity of DCX on cell survival against OGD, and the DCX induced upregulation of E-, VE- and N-cadherin, MAP2 and nestin. In NIH3T3 cells, DCX overexpression had no effect on cell survival against OGD, and indicating that the protective effects of DCX was restricted to brain cells e.g. SVZ and U-87 cells. Our data suggest a novel and an important role for DCX as a protective agent for migrating neuroblasts and tumor cells. © 2006 Published by Elsevier Ltd on behalf of IBRO.

Key words: neuroprotection, doublecortin, cadherin, MAP2, nestin, cell migration.

*Correspondence to: M. Chopp, Neurology Research, Henry Ford Hospital, Education and Research Building, Room 3056, 2799 West Grand Boulevard, Detroit, MI 48202, USA. Tel: +1-313-876-3936; fax: +1-313-876-1318.
E-mail address: chopp@neuro.hfh.edu (M. Chopp).

Abbreviations: CMV, cytomegalovirus; DCX, doublecortin; GFP, green fluorescent protein; hMSC, human marrow stromal cell; MAP2, microtubule-associated protein-2; MCAO, middle cerebral artery occlusion; MTS/PMS, modified tetrazolium/formazan; nestin-GFP, green fluorescent protein driven by nestin promoter; nt, nucleotide; OGD, oxygen and glucose deprivation; PBS, phosphate buffer saline; P-7, passage-7; P-20, passage-20; siRNA, small interfering RNA; SVZ, subventricular zone; T7, seven thymidines; VEGF, vascular endothelial growth factor; X-Gal, 5-bromo-4-chloro-3-indolyl P3-D-galactoside.

0306-4522/06$30.00+0.00 © 2006 Published by Elsevier Ltd on behalf of IBRO.
doi:10.1016/j.neuroscience.2006.06.065

Many adult stem or progenitor cells do not proliferate indefinitely, because of insufficient telomerase activity, telomere-independent senescence, cell death due to nontelomeric damage, or stress with expression or suppression of certain genes (Campisi 2005a,b). Doublecortin (DCX) is an X-linked gene located on Xq22.3-q23. It is evolutionarily conserved and a microtubule-associated protein that leads to microtubule organization or stabilization in migrating neuroblasts (Francis et al., 1999; Gleeson et al., 1999). Acute inactivation of DCX in rodents produces significant migration defects, although DCX knockout mice do not display a major disruption in migration (Bai et al., 2003; Corbo et al., 2002). In transgenic mice, overexpression of human Bcl-2 driven by the neuron-specific enolase promoter (NSE-huBcl-2) shows a significant reduction of apoptotic cells in the hippocampal granule cell layer as demonstrated by quantification of progenitor cells using DCX and new neurons using bromodeoxyuridine (BrdU)/neuronal nuclei antigen (NeuN) double-labeling (Kuhn et al., 2005). Combined treatment with human marrow stromal cells (hMSC) and a nitric oxide donor, (Z)-1-[N-(2-aminoethyl)-N-(2-ammonioethyl) aminio] diazen-1-ium-1,2-diolate (DETA/NONOate), increases angiogenesis, neurogenesis, DCX immunoreactive cells in the ischemic boundary area and neurological functional recovery after stroke in rats, subjected to permanent middle cerebral artery occlusion (MCAO) (Chen et al., 2004). When rats, subjected to MCAO, are treated with hMSC therapy, neurological recovery from stroke via induction and co-localization of insulin-like growth factor 1 and DCX in ischemic brain (Zhang et al., 2004b), indicates the involvement of DCX in neuroprotection. Downregulation of DCX expression in the ischemic boundary and attenuation of functional recovery after stroke in eNOS-deficient mice, subjected to permanent MCAO (Chen et al., 2005), also suggest that DCX plays a role in neuroprotection after stroke. Despite the above-noted studies, there is no report regarding the possible direct effect of DCX on cerebral neuroblasts.

Given that DCX is highly upregulated in subventricular zone (SVZ) cells after neural injury and stroke, we employed gene transfer technology and a tissue culture model system of SVZ cells subjected to a severe hypoxic condition of serum, oxygen, and glucose deprivation (OGD) to test whether DCX plays a role in neuroprotection. The introduction of DCX small interfering RNA (siRNA) into DCX expressing cells was utilized to knock down DCX expression in sequence-specific degradation of the RNA and to confirm the specificity of DCX on OGD. We propose that DCX confers neuroprotection to SVZ cells as they

migrate from the SVZ to the boundary of an ischemic lesion. In order to test the cell specificity of DCX as a protective agent, we also transfected the mouse NIH-3T3 and human U-87 glioma cells with DCX and measured survival under an adverse condition of OGD. Our data demonstrate that OGD-induced apoptosis in both SVZ cells and in human U-87 glioma was significantly inhibited by DCX synthesis.

EXPERIMENTAL PROCEDURES

All experimental procedures have been performed according to the U.S. National Institutes of Health Guide for the Care and Use of Laboratory Animals (NIH Publications No. 80-23) and approved by the Institutional Animal Care and Use Committee of Henry Ford Health System. All efforts were made to minimize the number of animals used and their suffering. Male Wistar rats (3–4 months of age) were used. The right MCAO was performed by placement of an embolus at the origin of the middle cerebral artery (Zhang et al., 1997).

Cell cultures

Human glioblastoma U-87 cells, mouse NIH3T3 and human embryonic kidney 293T cells obtained from American Type Culture Collection (Manassas, VA, USA) were maintained in DME supplemented with 5% fetal bovine serum (FBS), 2 mM glutamine, 100 U/ml penicillin and 50 μg/ml streptomycin. The SVZ of the adult male rat and mouse brain was examined under a microscope (Olympus BX40; Olympus Optical, Tokyo, Japan) and was surgically resected according to methods previously described (Wang et al., 2004). SVZ cells were dissociated in the medium containing 20 ng/mL of epidermal growth factor (EGF; R&D system, Minneapolis, MN, USA) and basic fibroblast growth factor (bFGF). Usually, rat SVZ cells in culture undergo senescence and cease proliferation after 15–20 passages *in vitro* based on radioactive [^{14}C] thymidine incorporation assay (Savarese et al., 2005; Pardo and Honegger, 2000). Two different passages of rat SVZ cells were chosen; a) passage-7, referred to as low (P-7) and proliferating SVZ cells, and b) passage-20 is referred to as long (P-20) and higher passage, senescent postmitotic cells. P-7 of rat SVZ cells was used for migration assay, and was infected with lentivirus to study the expression of E, VE, N-cadherin, microtubule-associated protein-2 (MAP2) and nestin.

β-Galactosidase staining

β-Galactosidase staining was performed according to method of Dimri et al. (1995). Briefly, SVZ cells were washed in PBS, fixed for 3 min in 3% formaldehyde, washed, and incubated at 37 °C for 16 h with fresh solution containing 1 mg of 5-bromo-4-chloro-3-indolyl P3-D-galactoside (X-Gal) per ml, 40 mM citric acid/sodium phosphate, pH 6.0, 5 mM potassium ferrocyanide, 5 mM potassium ferricyanide,150 mM NaCl and 2 mM MgCl2.

Construction of CMV-expression vector and stable transfection

Mouse DCX cDNA driven by CMV promoter was inserted into the expression vector pcDNA3.1A to generate stably transfected clones. Full-length mouse DCX cDNA from pYX-Asc library (ATCC) was digested with restriction endonuclease EcoR I and *Kpn*I and subcloned into pcDNA3.1Myc-His(−)A (Invitrogen Corporation, San Diego, CA, USA). The orientation of the insert was verified by restriction endonuclease digestion and DNA sequencing from Applied Genomics Technology Center, Wayne State University, Detroit, MI, USA. U-87 and NIH3T3 cells were stably transfected with the DCX expression vector (Fig. 1C). The U-87 cells (10^6) and mouse NIH3T3 cells (10^6) were transfected with 10 μg of purified DNA by Lipofectamine™ 2000 Reagent (Invitrogen) according to the manufacturer's protocol, and incubated at 37 °C in a humidified incubator for 12–16 h. Stably transfected cells were isolated and cultured routinely, as previously described (Santra et al., 1995). Five highly DCX expressing clones were pooled on the basis of real-time PCR data (data not shown). The

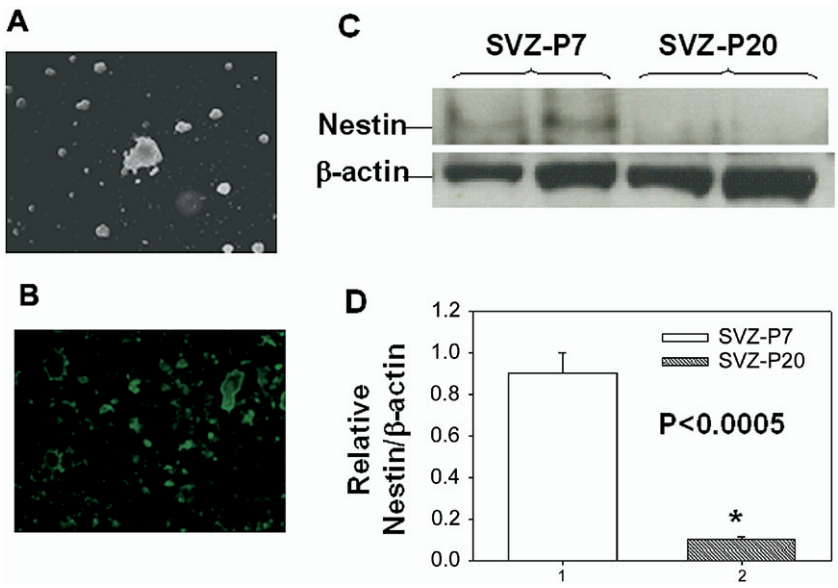

Fig. 1. β-Galactosidase staining and nestin expression in SVZ cells. SVZ (P-7) cells, (A) and SVZ (P-20) cells (B) are stained with X-Gal for β-galactosidase. Western blot analysis of nestin (C) in SVZ (P-7 and P-20) cells is performed. Migration of nestin and β-actin is marked in left. Quantitative analysis of nestin expression (D) in SVZ (P-7 and P-20) cells, is based on relative histogram per β-actin in three independent experiments. Asterisk indicates that there are significant differences between nestin expression in SVZ (P-20) cells, relative to SVZ (P-7) cells. Values of $P<0.05$ are considered significant.

pooled clones were used as DCX synthesizing U-87 and NIH3T3 cells.

Construction of lentivirus vector and virus infection

Decorin expressing lentivirus vectors with and without green fluorescent protein (GFP) expression cassette were digested with *Bam*H I and *Xba*I and the decorin insert was replaced with DCX cDNA fused to the 3′ end of the human cytomegalovirus (CMV) early gene promoter/enhancer from pcDNA-3 (Santra et al., in press). Briefly, the decorin expressing lentivirus vector has been made from decorin expressing vector pcDNA3 (Santra et al., 1995) and lentivirus vector pLV-TH (Wiznerowicz and Trono, 2003). Decorin cDNA including CMV promoter that drives decorin expression, was excised from decorin expressing vector pcDNA3 by restriction endonuclease digestion with *Bgl*II and EcoR I and ligated into lentivirus vector pLV-TH, digested with *Bam*H I and EcoR I. Here we removed decorin cDNA only by restriction endonuclease digestion with *Bam*H I and *Xba*I from decorin expressing lentivirus vectors with and without GFP expression cassette and ligated mouse DCX cDNA that was excised from DCX expression vector pcDNA3 (containing entire DCX cDNA including transcription start codon ATG and polyadenyl nucleotides, nt) digested with *Bam*H I from 5′ end of DCX cDNA (21 nt before ATG) and *Xba*I from pcDNA3 vector. The orientation of the inserts was verified by restriction endonuclease digestion and DNA sequencing from Applied Genomics Technology Center. The male adult rat SVZ cells are low transfection efficient cells. Rat SVZ cells (P-7) were infected with lentivirus carrying the DCX gene and lentivirus-only as control. All recombinant lentiviruses were produced by transient transfection of 293T cells and infected in SVZ cells, according to the method of Wiznerowicz and Trono (2003). Infection of virus was monitored by observing GFP expression under a fluorescent illumination microscope (Olympus IX71/IX51) by infecting the cells with GFP containing lentivirus. DCX expression was confirmed by real time PCR and Western blot analysis (Fig. 2).

DCX siRNA construct

To generate DCX siRNA-1, a 25 nt oligo (oligo 1) corresponding to nt 1–25 of DCX coding region was first attached to the 9-nt spacer (ttcaagaga) which had maximum efficiency to knock down p53 and CDH1 genes (Brummelkamp et al., 2002) and was followed by reverse complementary of oligo 1, seven thymidines (T7) as termination signal and endonuclease Mlu I sequence. The endonuclease *Cla*I was inserted at the both ends of DCX siRNA-1 to

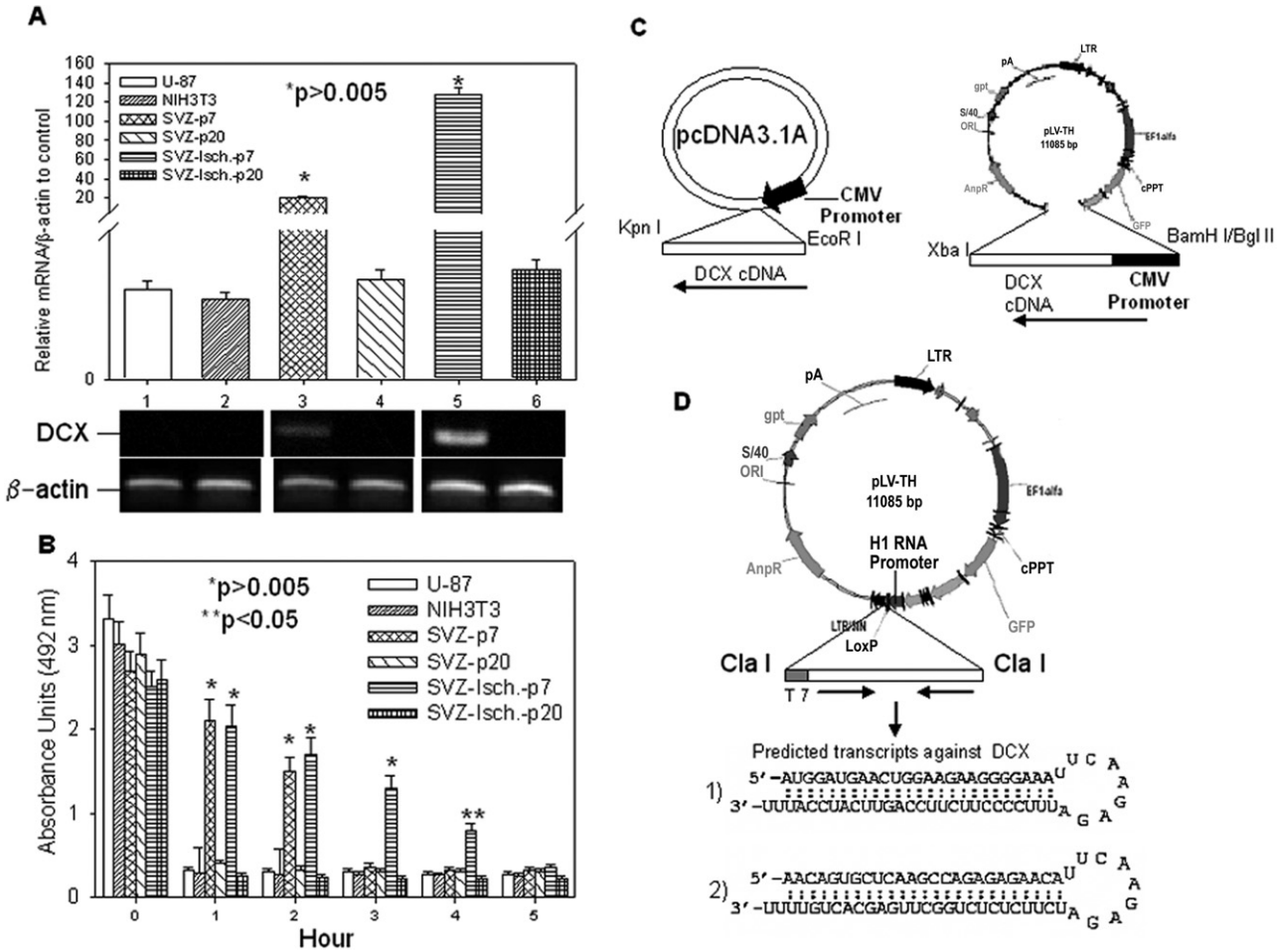

Fig. 2. DCX expression and proliferation assay in rat SVZ, NIH3T3 and human glioblastoma U-87 cells. DCX expression is analyzed by semi-quantitative real time PCR shown in top panel A, and DNA bands of PCR products are separated by 1.5% agarose gel in bottom panel A. Data are normalized to β-actin. Asterisks indicate that there are significant different in DCX expressing samples relative to NIH3T3 as control. Values of $P<0.05$ are considered significant. (B) Proliferation assay of cells from Fig. 1A followed by 5 h OGD. The number of viable cells is equivalent to absorbance units (492 nm) measured by using a modified nonradioactive MTS/PMS assay. (C) Constructs of DCX expression vector, pcDNA3.1A, DCX expression lentivirus vector, pLV-TH driven by CMV promoter. (D) Constructs of DCX siRNA expression lentivirus vector, pLV-TH driven by H1 RNA promoter.

Table 1. Sequences of DNA primers used in semi-quantitative real time PCR

Gene	Species	Sense	Anti-sense
DCX	Rat/mouse	ATGCAGTTGTCCCTCCATTC	ATGCCACCAAGTTGTCATCA
DCX	Rat/mouse	CTTTTGGTTCAGCAGAAGGG	CAAATGTTCTGGGAGGCACT
DCX	Human	TTGCCCTGTCTAATTTTGCC	AAAAGGGGCACTTGTGTTTG
DCX	Human	TTTCCAGATTCAATCAGCCC	AAAGATCTGCTGAGGGGGAT
E-cadherin	Human	GCTCAAGCTATCCTTGCACC	CTTGAGCCCAGGAGTTTGAG
E-cadherin	Rat	CTGAGGACTTTGGTGTGGGT	CTGGGTTAATCTCCAGCCAA
E-cadherin	Mouse	AACCAATGTTTTCTGGCTGG	TTAAATCGGCCAGCATTTTC
N-cadherin	Human	AGGATCAACCCCATACACCA	TGGTTTGACCACGGTGACTA
N-cadherin	Rat	CATCAATGGCAATCAAGTGG	CATACGTCCCAGGCTTTGAT
N-cadherin	Mouse	CTGGGACGTATGTGATGACG	TGATGATGTCCCCAGTCTCA
VE-cadherin	Human	TAATCACGATAACACGGCCA	GGCATCCCATTGTCTGAGAT
VE-cadherin	Rat	CACAGTAGATGGCAGCTGGA	CTGCCATGCTGCTTATGAAA
VE-cadherin	Mouse	CTTCAAGCTGCCAGAAAACC	ATTCGGAAGAATTGGCCTCT
MAP2	Human	GAAAGACGAAGCAAAGGCAC	CCCTGTATGGGAATCCATTG
MAP2	Rat	CAGAACATACCACCAGCCCT	TGAGTGAGGCTGATGTCCAG
MAP2	Mouse	GAGAAACGTTCTTCCCTCCC	GTGTGGAGGTGCCACTTTTT
Nestin	Human	GAAGAGAACCTGGGAAAGGG	TCTCCACCGTATCTTCCCAC
Nestin	Rat	TTAGCCACAAACCTCAACCC	TACCAGTTCCCAGATTTGCC
Nestin	Mouse	AGAGGACCAGGTGCTTGAGA	TCCTCTGCGTCTTCAAACCT

generate streaky ends for ligation into LVTH (Wiznerowicz and Trono, 2003). The following was the sequence of DCX siRNA-1.

5′-CGATATGGATGAACTGGAAGAAGGGGAAAttcaagaga TTTCCCCTTCTTCCAGTTCATCCATTTTTTTACGCGTAT-3′

DCX RNAi-2 was designed from a 25-nt oligo (oligo 2) corresponding to nt 149–163 of DCX coding region. It was separated by the above mentioned 9-nt spacer sequence (ttcaagaga) from reverse complementary of oligo 2, followed by T7 as termination signal and endonuclease Mlu I sequence. The endonucleases *Cla*I were incorporated at the both ends of DCX siRNA-2 like DCX siRNA-1. Sequence of DCX siRNA-2 was as follows.

5′-CGATGAACAGTGCTCAAGCCAGAGAGAACAttcaagag aTGTTCTCTCTGGCTTGAGCACTGTTTTTTTTACGCGTAT-3′

Sequences for siRNAs were analyzed by BLAST research to ensure that they did not have significant sequence homology with other genes. DCX siRNA-1 and 2 were hybridized with their respective reverse complementary stands to generate double stands DNA and ligated into pLV-TH digested with *Cla*I. The orientation of the inserts was verified by restriction endonuclease digestion and DNA sequencing from Applied Genomics Technology Center. The specific function of DCX on OGD was determined by using DCXsiRNA technology. Two DCXsiRNAs were inserted into the lentiviral vector pLV-TH driven by H1 RNA promoter (Fig. 1D). Efficiency of two DCXsiRNAs was based on analysis of DCX knockdown by quantitative real time PCR followed by infection with DCX siRNA lentivirus in DCX-transfected NIH3T3 clones. These two DCXsiRNAs mixtures were used in all experiments. Among six DCXsiRNAs constructs, these two successfully knocked down DCX expression. The other four DCXsiRNAs are not shown.

Cell treatment and induction of hypoxia

The cells were rinsed twice with serum free and glucose free media. The cells were incubated for different times with minimum volume of serum free and glucose free medium in hypoxia without oxygen in an airtight Plexiglas humidified chamber (Anaerobic Environment, Sheldon Manufacturing Inc., Cornelius, OR, USA), which was maintained at 37 °C and continuously gassed with a mixture of 99% N_2/1% CO_2/0% O_2. Cells were placed into this Sheldon hypoxia chamber on culture day 4 and remained there for 4–24 h.

Real-time semi-quantitative PCR, cell proliferation assays and TUNEL assay

The cDNA was synthesized by using Superscript III RT from total RNA, according to the manufacturer's protocol (Invitrogen). All DNA primers used are shown in Table 1. Real time PCR was performed in ABI Prism 7700 Sequence Detection System (Applied Biosystems, Foster City, CA, USA) by using SYBR Green PCR Master Mix (Applied Biosystems) for 2 min at 93 °C, followed by 28–36 cycles of 7 s at 93 °C, 30 s at 65 °C and 30 s at 70 °C, as described previously (Zhang et al., 2004b). Dissociation curves and agarose gel electrophoresis were used to verify the quality of the PCR products. Each sample was tested in triplicate using quantitative RT-PCR. All values were normalized to β-actin. Values obtained from five independent experiments were analyzed relative to gene expression data using the $2^{-\Delta\Delta CT}$ method (Livak and Schmittgen, 2001).

The CellTiter 96 Aqueous Non-Radioactive Cell Proliferation Assay (Promega Corporation, Madison, WI, USA) was used to determine the number of viable cells in the proliferative phase, according to the manufacturer's protocol. This nonradioactive cell proliferation assay is a colorimetric method based on a modified tetrazolium/formazan (MTS/PMS) assay (Santra et al., 1995). In this method, the amount of formazan product is time-dependent and proportional to the number of viable cells. TUNEL stains (Santra et al., in press) were performed by using the ApopTag Red Kits containing Digoxigenin/rhodamine conjugated anti-digoxigenin system (Intergen Company, Purchase, NY, USA), according to the manufacturer's protocol. Small DNA fragments diffused from the nucleus of the cells. TUNEL staining was confined to the nucleus or what appeared to be diffuse nuclear debris.

Cell migration assay

SVZ tissue explant. Adult male Wistar rats were subjected to the right MCAO, as previously reported (Zhang et al., 1997). The MCAO rats were killed after 2 weeks. The SVZ tissues were isolated from MCAO adult rats as previously described (Chen et al., 2005), cut into very small pieces and plated on Matrigel (BD Biosciences, San Jose, CA, USA) containing either 10^9 DCX lentivirus or DCX siRNA lentivirus or lentivirus particles/ml as control in 24 wells with neural basal-A medium containing 2% B27

supplement (Invitrogen) (Leventhal et al., 1999) and respective virus at the same concentration as in Matrigel. The average linear distance and the total area of cell migration from the explant culture edge were captured using a 10× objective (BX40; Olympus Optical) via the MCID computer imaging analysis system and measured at day 3 using the MCID software. The average of the 10 longest migration distances and the area encompassing migration were assessed in each explant culture. To examine the effect of DCX on SVZ cell migration, SVZ tissues from normal rat and rats subjected to MCAO were infected with lentivirus carrying DCX gene and empty lentivirus as control. In order to knock down endogenous DCX expression, DCX-infected SVZ tissues were treated with DCXsiRNA lentivirus.

Quantitative scrape migration for U-87. U-87 control and DCX-transfected cells were grown to complete confluence on a six-well plate. The scrapes were made by scratching with sterile 200 microliter pipette tip. Two hundred-microliter pipette tip scrapes correlate to a width 200×height 448 pixel areas. Such areas were selected from time 0 and 3 h pictures. Images were inverted, thresholded to eliminate background, and converted to binary (black and white) form, and an integrated density measurement was performed based on histogram. In essence, this method allowed the quantification of the amount of bright white refraction that accompanies the perimeter of each cell within the scrape area. Time 0 numbers were subtracted from 3 h calculations to provide a net migration into the wound. From three to six scrapes per treatment group were analyzed for each experiment. Five experiments were analyzed for quantification.

Immunohistochemistry and Western blot analysis

For immunohistochemistry, rat SVZ cells (P-7) were dissociated and plated on poly-L-ornithine/laminin-coated 96-well plates at a density of 10,000 cells/well. The 50,000 U-87 cells were seeded in eight-well chamber slides (Laboratory-Tek, Nunc, Inc., Naperville, IL, USA). After 2 days, SVZ and U-87 cells were washed with phosphate buffer saline (PBS) and fixed with 4% paraformaldehyde for 10 min on ice. Then cells were washed with PBS (4 °C) and stored at 4 °C. After permeabilization on ice using 0.1% Triton X-100 (Sigma-Aldrich) in PBS, cells were incubated with blocking solution (1% BSA in PBS) at room temperature for 1 h. Mouse monoclonal antibodies for VE- and N-cadherin (1:1000; Santa Cruz Biotechnology, Santa Cruz, CA, USA), for E-cadherin (1:1000; Transduction Laboratories Lexington, KY, USA), for MAP2 (1:1000; Chemicon International Inc., Temecula, CA, USA) and for nestin (1:1000; BD Pharmingen, San Diego, CA, USA) were incubated overnight at 4 °C. Cells were then washed with 0.1% BSA in PBS and incubated for 1 h with the anti-mouse secondary antibodies conjugated with fluorescein isothiocyanate (FITC) at room temperature. The cells were examined under a fluorescent illumination microscope (Olympus IX71/IX51) in five independent experiments. For Western blot analysis, cells were incubated in serum-free medium for 1.5 h, rinsed twice with PBS and harvested in ice-cold lysis buffer containing 50 mM Hepes pH 7.4, 1% Triton X-100, 10% glycerol, 150 mM NaCl, 2 mM EDTA, 10 mM NaF, 1 mM Na3VO4, 10 mg/ml leupeptin, 10 mg/ml aprotinin and 1 mM PMSF. Proteins (typically 40 μg) were directly subjected to SDS-PAGE, separated by SDS 10% PAGE, transferred onto nitrocellulose membranes, and blocked with 5% BSA for 18 h, and analyzed by immunoblotting with the indicated specific antibodies using the ECL detection system (Santra et al., 1995) in five independent experiments. Proteins were transferred onto a nitrocellulose membrane and incubated with goat anti-serum for DCX (1:1000; Santa Cruz Biotechnology) as primary antibody, and donkey anti-goat horseradish peroxidase antibody (Jackson ImmunoResearch Laboratories, West Grove, PA, USA) as secondary antibody. Mouse monoclonal antibodies (1:1000) for E, VE- and N-cadherin, MAP2, nestin and (β-actin, Santa Cruz Biotechnology) were used as primary antibody, and anti-mouse horseradish peroxidase antibody (1:10,000; Jackson ImmunoResearch Laboratories) as secondary antibody.

Statistical analysis

One-way analysis of variance (ANOVA) followed by Student-Newman-Keuls test was used. The values were the mean of 5 to 10 independent experiments for real-time PCR data and three independent experiments for Western blot analysis. The data are presented as mean±S.D. Values of $P<0.05$ are considered significant.

RESULTS

DCX expression in SVZ cells

A proliferation assay for mouse SVZ cells, using a MTS/PMS assay (Santra et al., 1995), demonstrated that the cells did not become senescent and continued to proliferate even after 60 passages (data not shown), as also reported by others (Pardo and Honegger, 2000; Reynolds et al., 1992). Thus, unlike mouse SVZ cells that proliferate indefinitely (Pardo and Honegger, 2000; Reynolds et al., 1992), in our laboratory adult rat SVZ cells in culture typically undergo replicative postmitotic senescence after 15–20 passages, which is in agreement with results of other studies (Savarese et al., 2005; Pardo and Honegger, 2000). Senescence-associated β-galactosidase staining was performed to confirm the senescence-associated rat SVZ cells after P-20 (Fig. 1A and B). The SVZ (P-7) cells were not stained with X-Gal (Fig. 1A) indicating that these cells did not express β-galactosidase and were dividing cells. In contrast, higher passage (P-20) SVZ cells were senescence-associated β-galactosidase positive, because they contained senescent SVZ cells as well as many post-proliferative astrocytes, which could abundantly express senescence-associated β-galactosidase (Evans et al., 2003). We examined the expression of nestin as a marker for migrating immature neuroblasts (Feuer et al., 2005; Glass et al., 2005), in SVZ cells. SVZ (P-7) cells maintained linear expression of nestin based on protein loading as shown in β-actin expression (Fig. 1C). In contrast, SVZ (P-20) cells were almost nestin negative and there was no linearity on nestin expression (Fig. 1C). Quantitative analysis of nestin expression showed that level of nestin in SVZ (P-7) cells was approximately ninefold higher than that in SVZ (P-20) cells (Fig. 1D). These data indicate that the proliferating SVZ (P-7) cells express nestin spontaneously. In contrast, nestin expression was almost undetectable in senescent postmitotic SVZ (P-20) cells.

To test cell survival and DCX expression, we compared low passage neural precursors SVZ (P-7) cells with higher passage, senescent postmitotic SVZ (P-20) cells from adult male rats. These cells were subjected to OGD. SVZ cells from adult male rats subjected to MCAO showed very high DCX mRNA expression based on real time PCR compared with normal proliferating SVZ cells (P-7) (Fig. 2A). In contrast, there was no DCX expression in both normal and ischemic senescent postmitotic SVZ (P-20) (Fig. 2A). The human glioblastoma cell line U-87 and mouse NIH3T3 were also used to determine the cell spec-

ificity of DCX expression. There was no detectable DCX expression in U-87 cells and NIH3T3 cells. These data suggest that DCX is an unstable hypoxic inducible gene. In order to examine the involvement of DCX in hypoxia, an OGD tissue culture model system was employed. The senescent postmitotic rat SVZ cells (P-20) both from normal rats and rats subjected to MCAO, became vulnerable and sensitive to OGD (Fig. 2B). Low passage neural precursors SVZ (P-7) cells with higher passage, senescent postmitotic SVZ (P-20) cells were subjected to OGD from 2 to 4 h and cell viability was measured using a MTS/PMS assay (Santra et al., 1995). Proliferating rat SVZ cells (P-7) from ischemic rat survived for 4 h after OGD (Fig. 2B). Normal proliferating rat SVZ cells (P-7) remained viable only after 2 h OGD. In contrast, both normal and ischemic senescent postmitotic rat SVZ cells (P-20) did not survive for 1 h. These data suggest that DCX expression may contribute to the survival of SVZ cells under OGD condition. To further test the effect of DCX on SVZ cells subjected to OGD, gene transfer technology was employed.

De novo DCX expression

Ectopic DCX expression was analyzed by real time PCR (Fig. 3A) at the mRNA level and by Western blot immunodetection technique at the protein level (Fig. 3B). The high DCX expressing clones were isolated on the basis of real time PCR. Five high DCX expressing clones were pooled and expressed DCX at the mRNA (Fig. 3A) and protein levels (Fig. 3B). These pooled clones were used in all experiments. When DCX overexpressing SVZ, U-87 and NIH3T3 were infected with the pooled DCX siRNA lentiviruses 1 and 2 (Fig. 2D), DCX expression was significantly knocked down both at the mRNA (Fig. 3A) and protein levels (Fig. 3B). These DCX overexpressing SVZ, U-87 and NIH3T3 cells were subjected to OGD to determine the direct effect of DCX on cell survival against OGD.

DCX upregulation protects brain cells against serum, OGD

SVZ, U-87 and NIH3T3 cells with and without DCX overexpression were incubated in OGD conditions for different times. The cell viability was measured by MTS/PMS assays from five individual experiments. The overexpressing SVZ and U-87 cells remained viable against OGD up to 32 h (Fig. 4). In contrast, control cells without ectopic DCX expression survived up to 2 h (Fig. 4). When these DCX overexpressing SVZ and U-87 cells were infected with the pooled DCX siRNA lentivirus, the cell viability was reduced very significantly after 2 h and 4 h of OGD (Fig. 4). These data suggest that DCX was directly and specifically involved in protection of SVZ and U-87 cells against OGD. Interestingly, DCX overexpressing NIH3T3 cells did not survive as long as DCX synthesizing SVZ and U-87 cells did. DCX overexpressing NIH3T3 cells remained viable for 4 h (Fig. 4). These data demonstrate that DCX protected brain cells e.g. SVZ and U-87 cells, but not mouse fibroblast NIH3T3 cells against OGD.

Anti-apoptotic effect of DCX

In order to test whether DCX synthesis reduces apoptosis after OGD, TUNEL assay was performed. Almost all control U-87 and SVZ cells (P-7) underwent apoptosis after

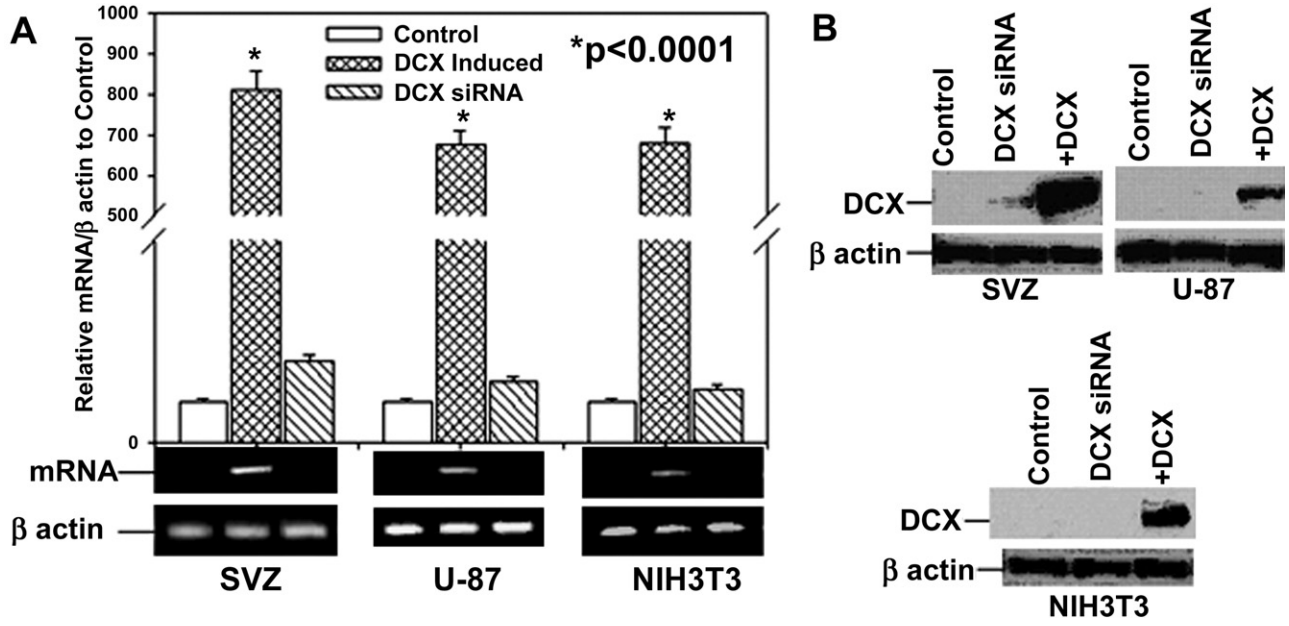

Fig. 3. Ectopic DCX expression in rat SVZ (P-7), human glioblastoma U-87, and NIH3T3 cells. The expression of DCX is analyzed by semi-quantitative real time PCR shown in the top panel A and DNA bands of PCR products are separated by 1.5% agarose gel in bottom panel A. Data are normalized to β-actin. Asterisks indicate that there are significant differences between DCX expressing samples relative to vector control. Values of $P<0.05$ are considered significant. (B) An immunoblotting analysis of total cell lysates from the different cells as indicated in the bottom of the gels by using an anti-DCX antibody and chemiluminescence. Loading of different samples is indicated in the top of the gels. The migrations of DCX and β-actin are marked on the left.

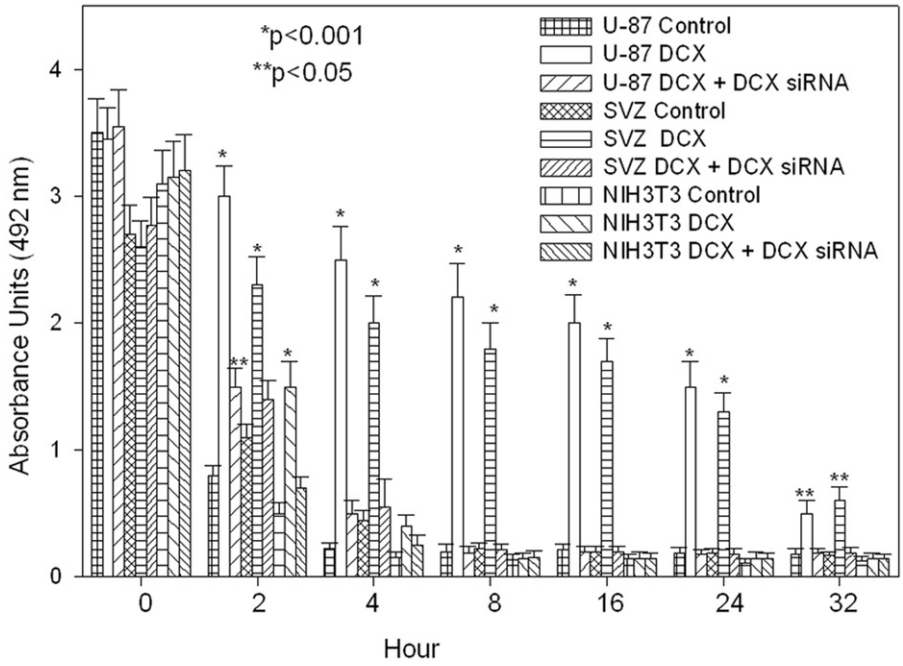

Fig. 4. De novo DCX synthesis induces cell survival against OGD in rat SVZ (P-7) and U-87 cells, but not in NIH3T3 cells. The number of proliferating cells is established by using a nonradioactive MTS/PMS assay. The U-87 and NIH3T3 cells transfected with empty pcDNA-3.1A vector as control, DCX expression vector transfected U-87 and NIH3T3 cells as DCX, rat SVZ cells (P-7) infected with empty lentivirus as SVZ control and rat SVZ cells (P-7) infected with DCX expressing lentivirus as SVZ DCX, the cells infected with DCX siRNA as +DCX siRNA are subjected to OGD for 2–32 h. Asterisks indicate that there are significant differences between DCX expressing samples relative to vector control. Values of $P<0.05$ are considered significant.

OGD. In contrast, DCX expressing cells had very faint fluorescent intensity indicating less apoptosis (~1%) based on cell count under a fluorescent illumination microscope (Olympus IX71/IX51) in five independent experiments (Fig. 5). These data suggest that DCX synthesizing cells were resistant to apoptosis after 6 h of OGD. In order to investigate the specificity of DCX against apoptosis, we utilized DCX SiRNA lentivirus with GFP expression. DCX expressing cells, infected with DCX SiRNA lentivirus containing GFP showed intense yellow fluorescence merged with red fluorescence from apoptosis and green fluorescence from GFP containing DCX SiRNA lentivirus (Fig. 5). These data indicate that only those cells that were infected with DCX SiRNA lentivirus and lost DCX expression, underwent apoptosis. These data strongly demonstrate that DCX protected these SVZ and U-87 cells against apoptosis after 6 h of OGD. Ectopic DCX expression revealed morphological diversity of the U-87 and SVZ cells, which were aggregated after 4 h of severe OGD (Fig. 5).

DCX promotes SVZ and U-87 cell migration

SVZ cells migrate toward ischemic area and may replace dead cells after MCAO (Zhang et al., 2001; Arvidsson et al., 2002; Lichtenwalner and Parent, 2006; Jin et al., 2001, 2003; Parent et al., 2002). SVZ tissue explant experiment shows that DCX lentivirus infection significantly enhanced SVZ cell migration (Fig. 6A, B) in both normal and MCAO SVZ tissues. In contrast, DCXsiRNA infection almost completely blocked SVZ cell migration (Fig. 6A, B). These data indicate that DCX was directly involved in SVZ cell migration. SVZ cells from the tissue of rats subjected to MCAO migrated significantly faster than from normal tissue (Fig. 6A, B). These data also are consistent with the observation that SVZ cells from rats subjected to MCAO expressed more DCX than the SVZ cells from normal rat (Fig. 2A, B). DCX, therefore, may facilitate migration of SVZ cells from the adult rat.

In the quantitative scrape migration assay, DCX-transfected U-87 cells completely occupied the empty space for 3 h while control cells just started migration (Fig. 6C, D). Treatment with DCXsiRNA significantly reduced migration by ~37% (Fig. 6C, D). These data show that DCX synthesis significantly increased cells migration.

Ectopic expression of DCX is associated with marked induction of N-cadherin, E-cadherin and VE-cadherin

N-, E-, and VE-cadherin are involved in cell migration, resistance to apoptosis (Li et al., 2001; Carmeliet et al., 1999) and protection against ischemia (Linke et al., 2005). In order to investigate the neuroprotective mechanism of DCX, using quantitative real time PCR, Western blot analysis and immunohistochemistry we measured the effect of DCX on N-, E-, and VE-cadherin expression in the proliferating stage of cells without OGD. Quantitative real time PCR and Western blot analysis showed that DCX greatly upregulated E-, VE- and N-cadherin in SVZ and U-87 cells (Fig. 7). For quantitative analysis of E-, VE- and N-cadherin, real time PCR data for mRNA and histogram data for protein were normalized to β-actin. E-, VE- and N-cadherin

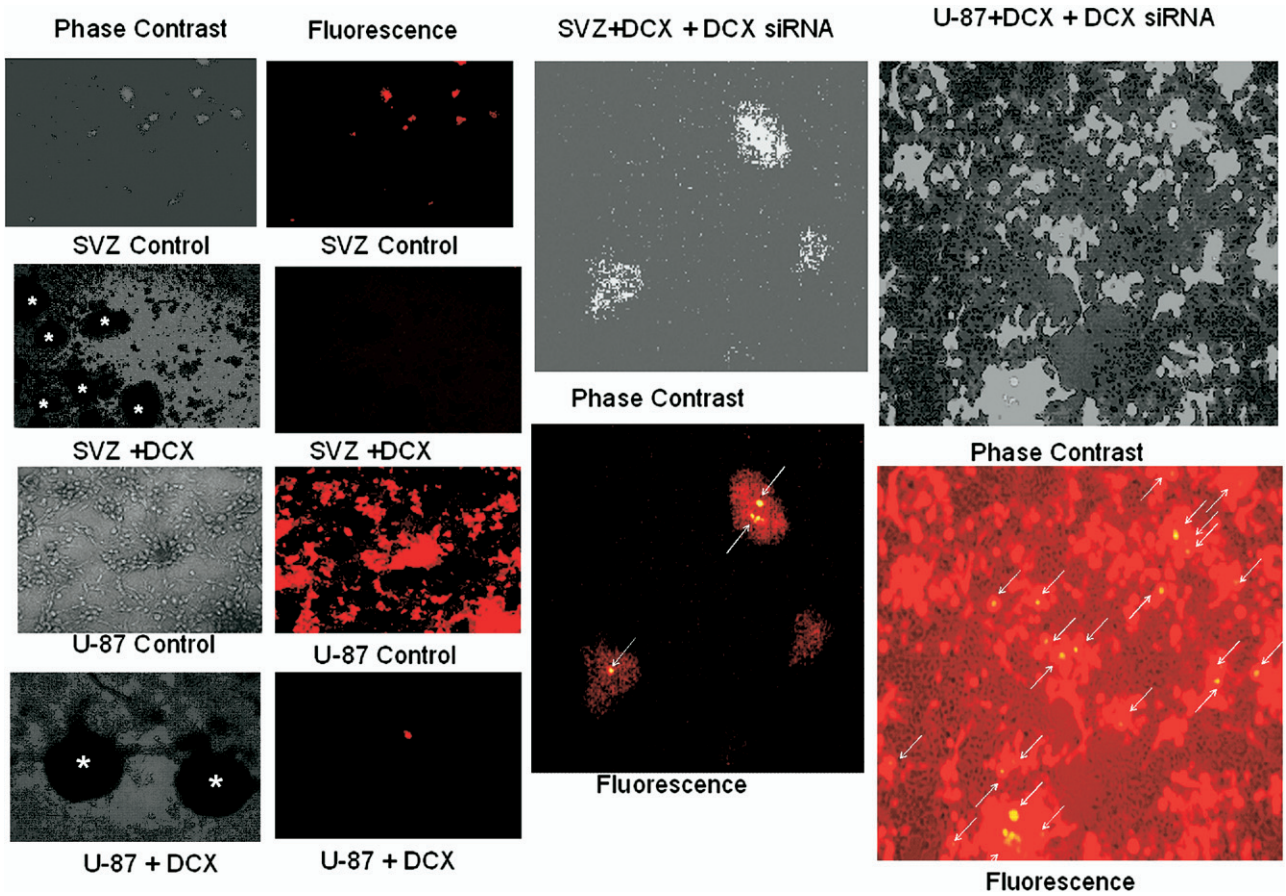

Fig. 5. De novo DCX expression protects rat SVZ (P-7) and U-87 cells from apoptosis. Cell death was detected by TUNEL staining as red fluorescence. The U-87 cells transfected with empty pcDNA3.1A vector as U-87control, DCX expression vector transfected U-87 cells as U-87+DCX, rat SVZ cells (P-7) infected with empty lentivirus without GFP as SVZ control and rat SVZ cells (P-7) infected with DCX expressing lentivirus without GFP as SVZ+DCX, and the cells infected with DCX siRNA with GFP expression as +DCX siRNA are subjected to 6 h OGD. Note that DCX expressing cells, infected with DCX SiRNA lentivirus containing GFP showed very significant yellow fluorescence merged with red fluorescence from apoptosis and green fluorescence from GFP containing DCX SiRNA lentivirus. Merging yellow fluorescence is indicated by arrow; 100% of control cells are apoptotic. In contrast, less than 1% of DCX expressing cells are apoptotic. Ectopic DCX expression reveals morphological diversity of the U-87 and SVZ cells which are aggregated, as indicated by asterisks during the incubation in severe OGD.

were upregulated by 2.5- to 5-fold (Fig. 7). DCX siRNA infection significantly reduced the level of E-, VE- and N-cadherin in DCX synthesizing cells by 20–40%. These data indicate that DCX induced E-, VE- and N-cadherin upregulation specifically in SVZ (P-7) and U-87 cells. In contrast, DCX had no effect on the regulation of E-, VE- and N-cadherin in NIH3T3 cells (Fig. 7). These data strongly suggest that DCX upregulates E-, VE- and N-cadherin specifically in brain cells e.g. SVZ and U-87 cells, but not in NIH3T3. In order to localize the E-, VE- and N-cadherin expression and to determine the morphological changes mediated by DCX in SVZ and U-87 cells, immunohistochemistry was performed.

Immunohistochemistry of E-, VE- and N-cadherin

The control U-87 and SVZ cells (P-7) maintained their wild-type morphology (Fig. 8). There was no detectable fluorescence in these corresponding control U-87 and SVZ cells, immunostained with antibodies against E-, VE- and N-cadherin (Fig. 8). DCX overexpressing U-87 cells turned into elongated endothelial-like cells (left panel) and DCX synthesizing SVZ cells aggregated, as observed in the phase contrast microscope (Fig. 8). Immunostaining of DCX overexpressing SVZ and U-87 cells with antibodies against E-, VE- and N-cadherin, showed very dense fluorescence where the cells were aggregated (Fig. 8). DCX expressing SVZ and U-87 cells induced cell aggregation and sphere formation. DCX synthesizing U-87 cells changed their morphology into an elongated shape. To investigate specifically how DCX acted on E-, VE- and N-cadherin expression, DCX overexpressing cells were infected with DCX-siRNA. Immunostaining for E-, VE- and N-cadherin was almost completely abrogated (Fig. 8) and the morphology of DCX expressing U-87 cells returned to the wild-type shape (Fig. 8).

Effect of DCX on MAP2 and nestin expression

Co-expression and regulation of MAP2 with E- and N-cadherin and neural cell adhesion molecule (N-CAM) are found in adult and fetal normal pituitary tissues (Rubinek et

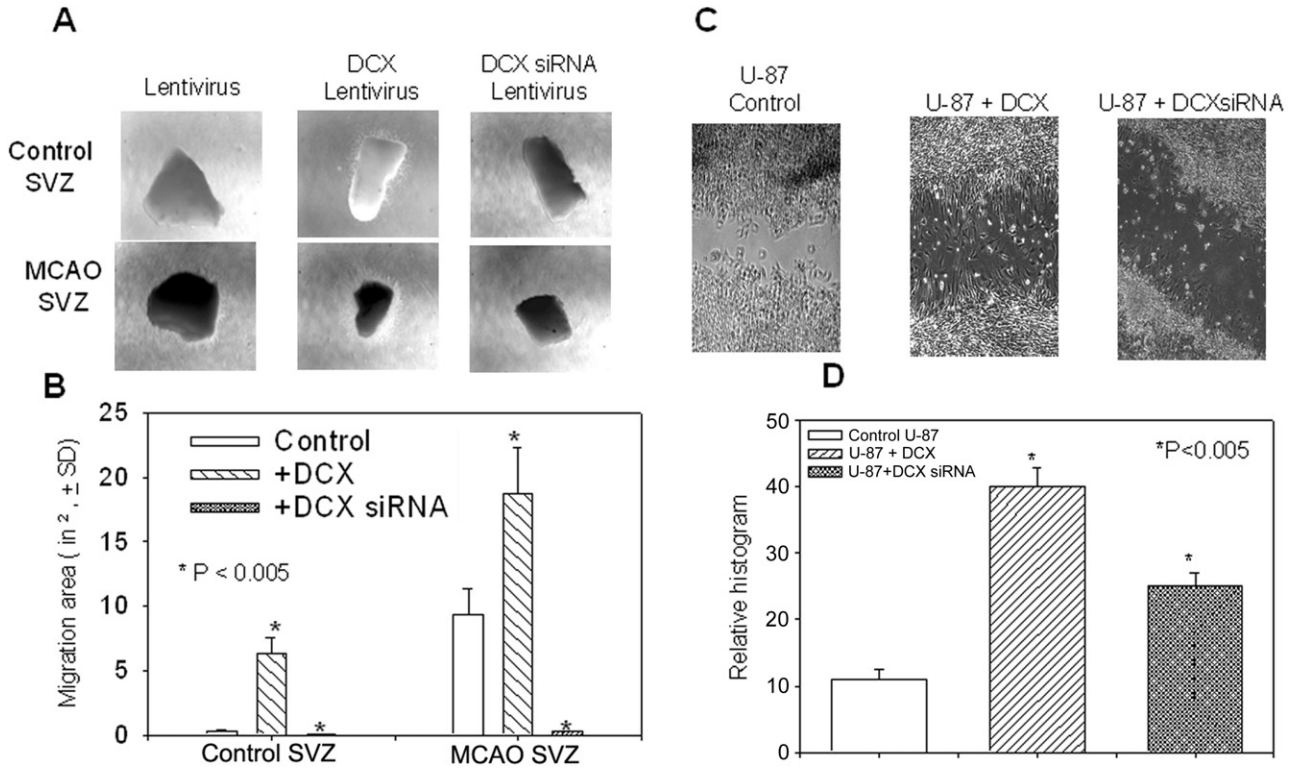

Fig. 6. DCX induces cell migration in SVZ tissue explant and U-87 cells. SVZ tissue explant migration assay was performed from normal adult rat in upper panel (A) and MCAO adult rat as a second row in the upper panel (A). The tissues are marked in the left, and lentivirus infections indicated in the upper figure (A). The bottom panel left (B) is quantitative analysis of cell migration by using a 10× objective (BX40; Olympus Optical) via the MCID computer imaging analysis system and measured at day 3. The upper right panel (C) is scrape migration assay for U-87 control, DCX-transfected U-87 cells and DCX-transfected U-87 cells infected with DCXsiRNA. The bottom panel right (D) is a quantitative analysis of cell migration by using a 10× objective (BX40; Olympus Optical) based on histogram analysis.

al., 2003), in primary cell culture, such as hippocampal progenitor cells (Amoureux et al., 2000), and even in teratocarcinoma cell line, such as mouse P-19 (Hamada-Kanazawa et al., 2004). MAP2 is a potent neuroprotective

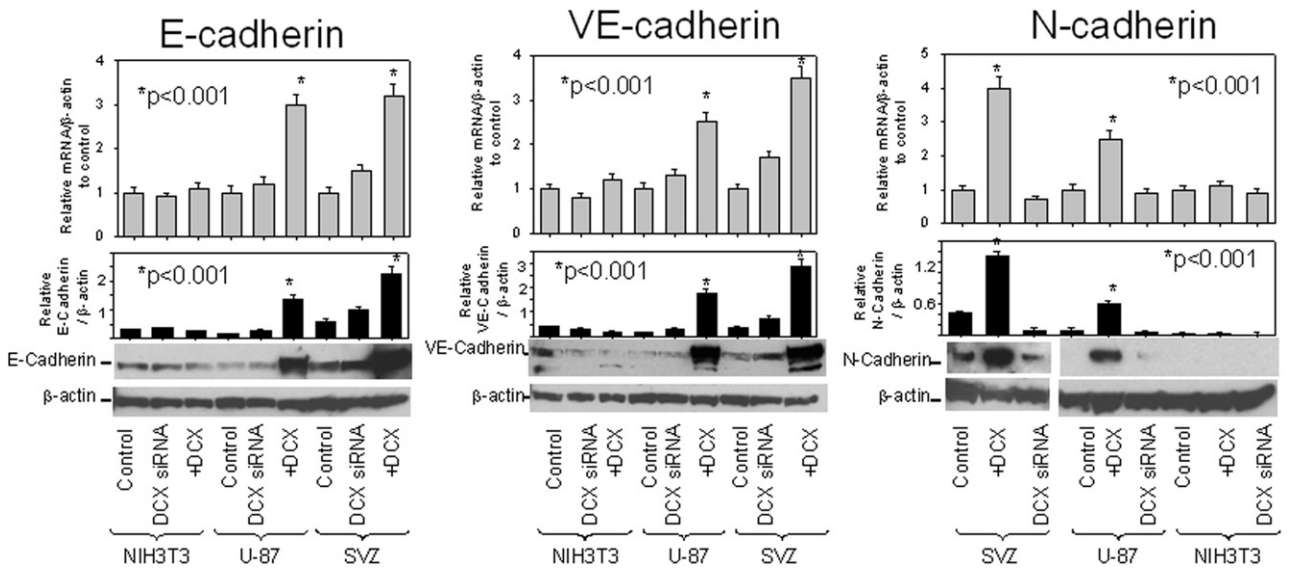

Fig. 7. Effect of DCX on E-, VE- and N-cadherin expression in NIN3T3, U-87 and rat SVZ (P-7) cells. Western blot analysis of the proteins from control, DCX expressing, DCXsiRNA-infected DCX expressing NIH3T3, U-87 cells and rat SVZ cells (P-7) is shown in the bottom panel. Migrations of proteins are indicated on the left. Quantitative real time PCR for mRNA and quantitative histogram analysis of Western blot for protein from three independent experiments are shown on the top of the gel for corresponding lane. Loading of the gel is indicated in the bottom. Note that E-, VE- and N-cadherin are upregulated 2.5- to 5-fold by DCX and are knocked down 60–80% by DCXsiRNA.

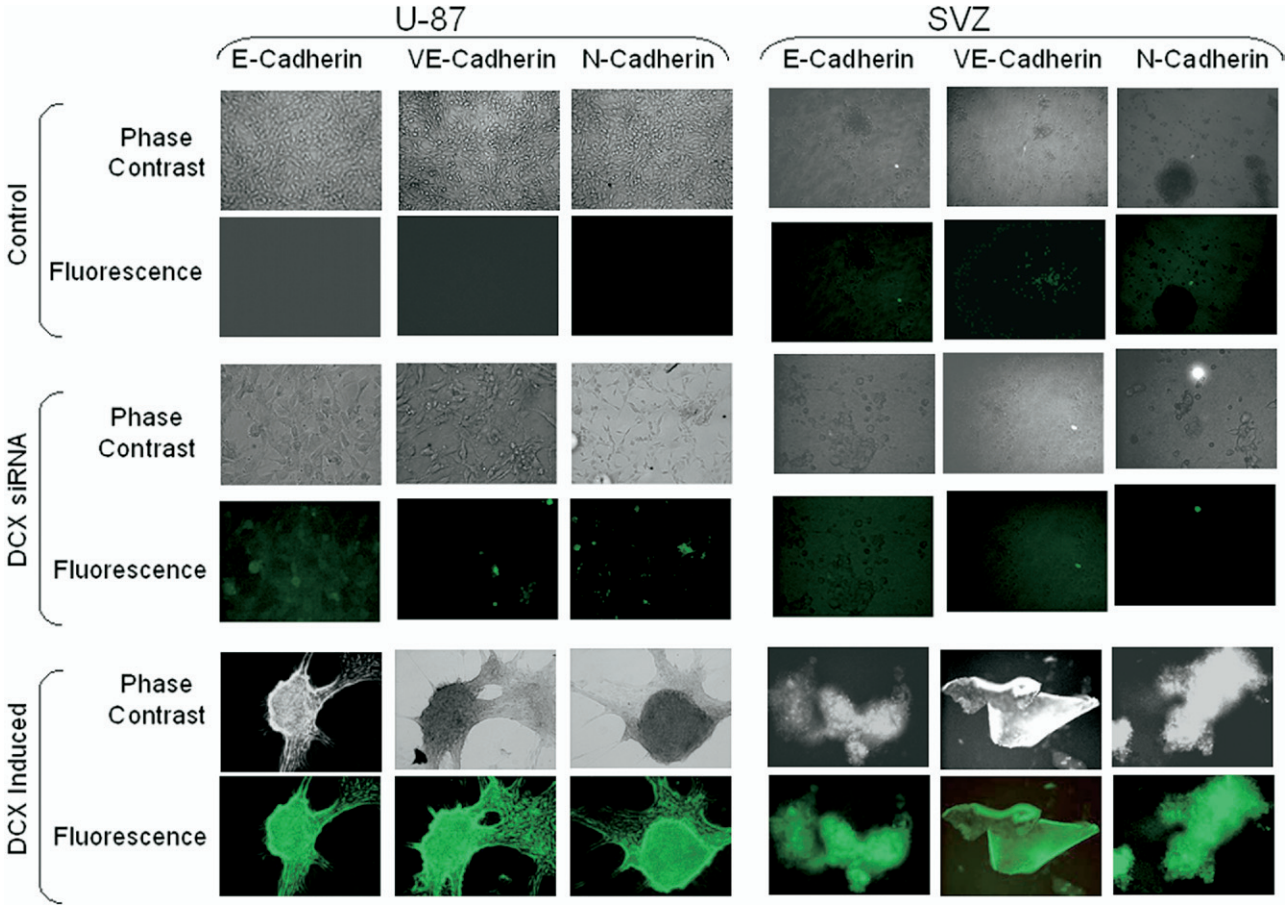

Fig. 8. Immunohistochemistry analysis of E-, VE- and N-cadherin expression in rat SVZ (P-7) and U-87 cells with and without DCX synthesis. Name of the cells and antibodies is indicated on the top. DCX transfections, infections, microscopic observations are indicated on the left. Note, that DCX expressing U-87 and SVZ cells are very positive with antibodies of E-, VE- and N-cadherin.

candidate against ischemic insult (Krugers et al., 2000; Ikeda et al., 1999; Yu et al., 2002; Hutter-Paier et al., 1998). Overexpression of N-cadherin upregulates nestin mRNA in P-19 cells (Gao et al., 2001). Nestin is also a hypoxia inducible gene (Chen et al., 2005; Glass et al., 2005; Yu et al., 2002). Using quantitative real time PCR, Western blot analysis and immunohistochemistry, we therefore examined whether DCX induced MAP2 and nestin expression after 12 h OGD. The data showed that DCX overexpression caused MAP2 and nestin expression in SVZ (P-7) and U-87 cells (Figs. 9 and 10). For quantitative analysis of MAP2 and nestin, real time PCR data for mRNA and histogram data for protein were normalized to β-actin. MAP2 and nestin were upregulated by two- to threefold (Fig. 9). DCX siRNA treatment significantly reduced MAP2 and nestin expression in DCX synthesizing cells by 20–40% (Fig. 9). In contrast, there was no MAP2 and nestin expression in DCX expressing NIH3T3 cells (Fig. 9). When DCX overexpressing SVZ (P-7) and U-87 cells were treated with DCX siRNA, MAP2 and nestin expression was abolished (Figs. 9 and 10). These data demonstrate that DCX may also protect SVZ and U-87 cells from OGD by inducing MAP2 and nestin expression.

DISCUSSION

In tissue culture, when brain cells are exposed to combined hypoxia and hypoglycemia in the presence of the glucose substitute, 2-deoxyglucose, they survive only for 6 h (Lyons and Kettenmann, 1998). Brain cells such as astrocytes and oligodendrocytes from rat and mouse also could not survive for more than 4 h of OGD (data not shown). Brain cells such as adult mouse SVZ and U-87 cells completely lose their cell viability after 4 h of OGD (Santra et al., in press). Decorin synthesis protects mouse SVZ cells and U-87 up to 24 h of OGD (Santra et al., in press). Here, we demonstrate the DCX overexpressing SVZ and U-87 cells remained viable after 32 h of exposure of severe OGD. In contrast, control SVZ and U-87 cells survived less than 4 h of OGD (Figs. 3, 4). NIH3T3 cells were unable to survive for more than 4 h even with overexpression of DCX. These data suggest that DCX is a brain specific gene that protects brain cells e.g. SVZ and U-87, but not mouse fibroblast NIH3T3. Apoptosis analysis showed that DCX protected the majority of SVZ and U-87 cells from apoptosis against OGD. Infection with DCX siRNA induced apoptosis specifically in those cells that had lost DCX expression.

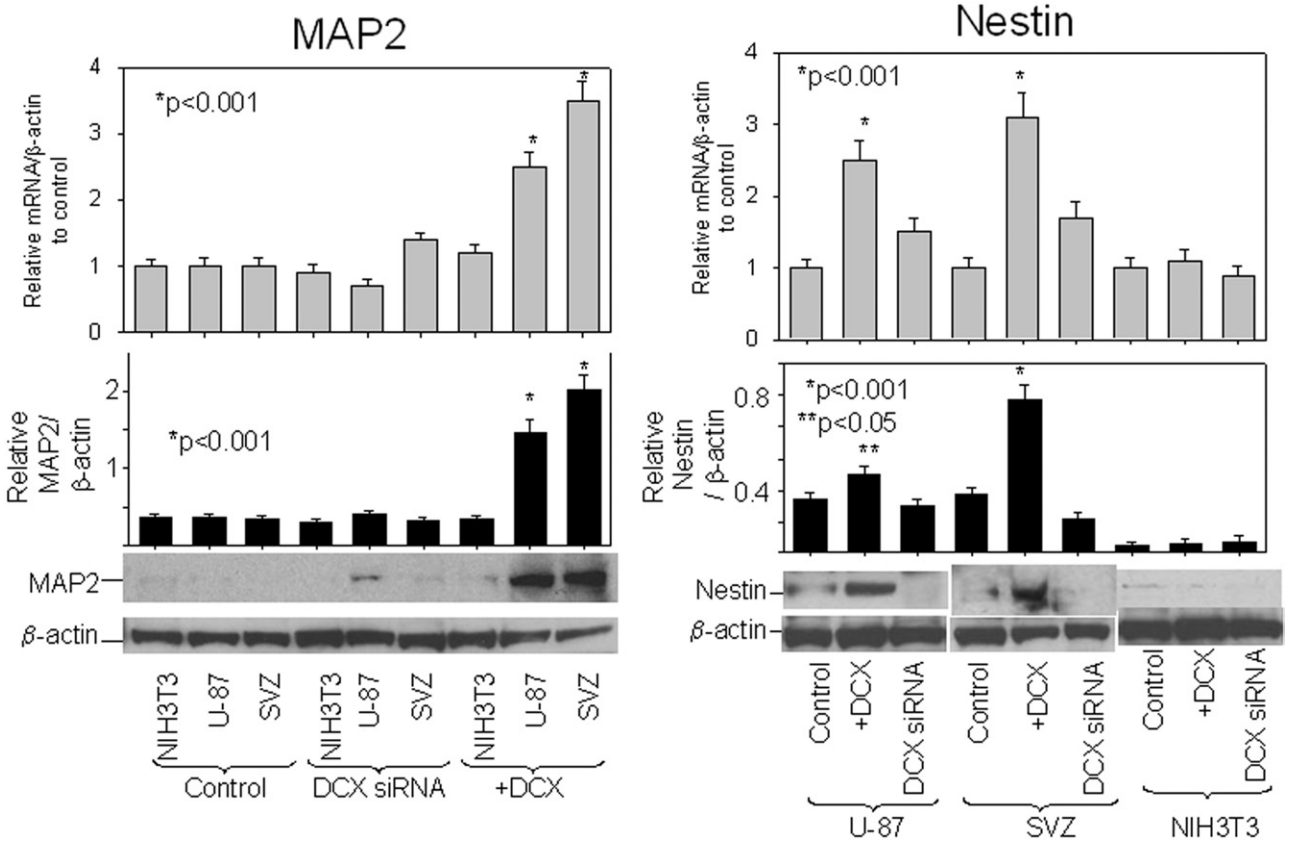

Fig. 9. Effect of DCX on MAP2 and nestin expression in NIN3T3, U-87 and rat SVZ (P-7) cells. Quantitative real time PCR for mRNA and quantitative histogram analysis of Western blots for protein from control, DCX expressing and DCXsiRNA-infected DCX expressing NIH3T3, U-87 and rat SVZ cells (P-7) of three independent experiments are shown in the upper panel and central panel respectively. Western blot analysis of the proteins is shown in the bottom panel. Migrations of proteins are indicated on the left. Loading of the gel is indicated in the bottom. Note, that MAP2 and nestin are upregulated two- to threefold by DCX and are knocked down with DCXsiRNA by 60–80%.

SVZ cells extracted from the adult male rat subjected to MCAO expressed significantly more DCX than normal SVZ cells. These ischemic SVZ cells migrated faster than normal SVZ cells, as shown in the tissue-explant migration assay. When DCX was overexpressed, SVZ cells from normal as well as rats subjected to MCAO and U-87 cells migrated faster than the wild-type cells. DCX induced cell aggregation in SVZ cells and cell enlargement in U-87 cells. Cell aggregation is also reported to be induced by cadherins (Navarro et al., 1998; Li et al., 2001; Charalambous et al., 2005). In our experiment, DCX-mediated E-, VE- and N-cadherins showed dense immunostaining specifically in a spherical area where the cells aggregated. Treatment with DCX siRNA abrogated their E-, VE- and N-cadherin expression and these cells resembled isolated and non-aggregated wild-type cells. These data demonstrate that DCX-induced E-, VE- and N-cadherin expression in SVZ and U-87 cells plays a role in the aggregation of SVZ cells and the enlargement of U-87 cells. Deficiency or truncation of VE-cadherin induces endothelial cell apoptosis associated with downregulation of *Bcl*II, and upregulation of the proapoptotic mediator p53 and abolishes transmission of the endothelial survival signal via vascular endothelial growth factor (VEGF)-A/AKT/phosphoinositide 3-kinase (PI3-K)/VEGF receptor-2/β-catenin (Carmeliet et al., 1999). Thus, VE-cadherin/β-catenin signaling may control survival of SVZ and U-87 cells from OGD. N-cadherin-mediated cell adhesion activates antiapoptotic protein AKT/PKB and subsequently increases β-catenin and inactivates the proapoptotic factor Bad in melanoma cells (Li et al., 2001). Thus, DCX promotes robust survival of SVZ and U-87 cells against OGD by upregulating E-, VE- and N-cadherin.

MAP2 binds microtubules through specialized microtubule-binding domains and increases microtubule polymerization that is involved in neuronal migration, dendritic outgrowth and synaptic plasticity. Treatment with metyrapone (Krugers et al., 2000), erythropoietin and cerebrolysin (Yu et al., 2002; Hutter-Paier et al., 1998) induces MAP2 expression and protects the cells from ischemic damage. Our data showed that DCX synthesis upregulated MAP2 in SVZ and U-87 cells. Induction of MAP2 by DCX may protect cells against OGD. SOX6 transfection induces E- and N-cadherin and MAP2 and promotes neuronal differentiation by stimulating cellular aggregation and cell to cell interaction in MAP2-null P19 cells (Hamada-Kanazawa et al., 2004). In our data, DCX-induced upregulation of MAP2 in SVZ and U-87 cells may be regulated via the SOX6/E- and N-cadherin signal pathway. These two MAPs, DCX and MAP2, may also be involved in neuronal migration in

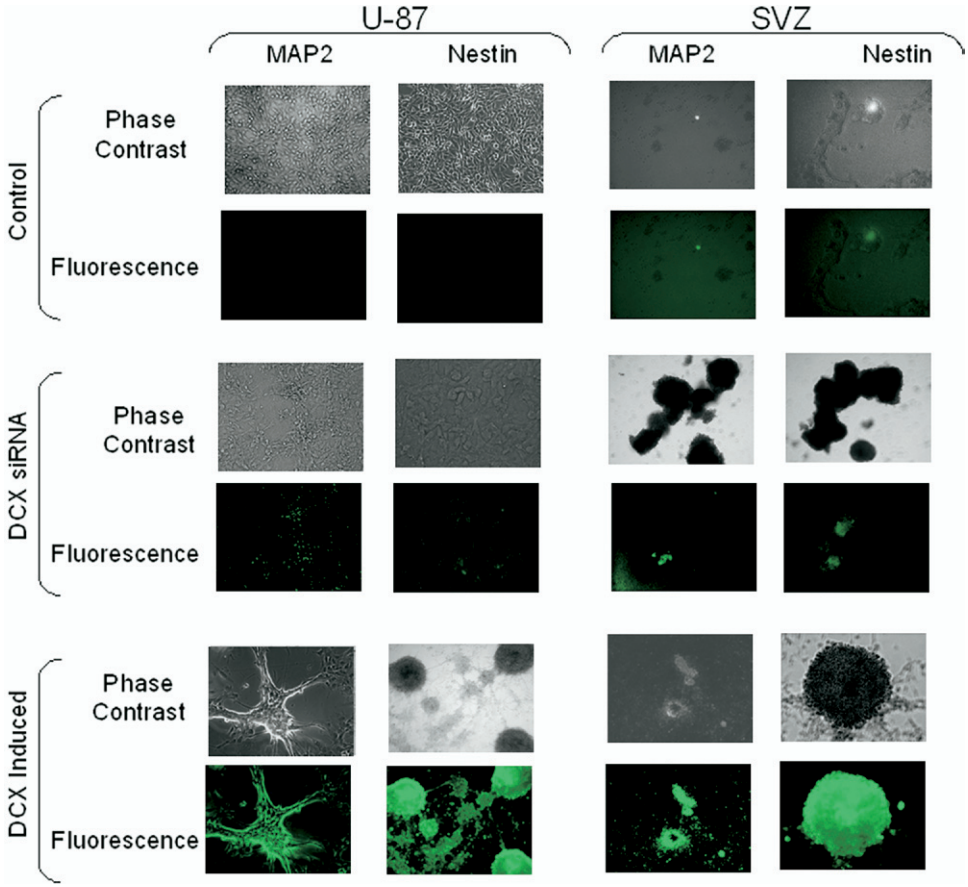

Fig. 10. Immunohistochemistry analysis of MAP2 and nestin expression in rat SVZ (P-7) and U-87 cell with and without DCX synthesis. Name of the cells and antibodies is indicated on the top. DCX transfections, infections, microscopic observations are indicated on the left. Note, that DCX expressing U-87 and SVZ cells are very positive against antibodies of MAP2 and nestin.

the same pathway as Tau and MAP1B promote neuronal migration (Takei et al., 2000), and MAP2 and MAP1B act synergistically to increase neuronal migration and dendritic extension (Teng et al., 2001). In addition, the absence of both MAP2 and MAP1B leads to perinatal lethality, reduced dendritic and total subunits of cAMP-dependent protein kinase (PKA) in hippocampal tissue and cultured neurons and reduced activation of cAMP-responsive element binding protein (Harada et al., 2002).

N-cadherin overexpressing P-19 cells induce nestin and Wnt1 expression (Gao et al., 2001). In our data, induction of nestin in SVZ and U-87 cells by DCX may be regulated by Wnt1/N-cadherin signal pathway. In a murine experimental glioblastoma model, endogenous neural precursors migrate from the SVZ toward the tumor and surround it (Zhang et al., 2004c; Glass et al., 2005). When red fluorescent protein-labeled murine glioblastoma G261 cells are implanted into the caudate-putamen of transgenic mice, which express green fluorescent protein driven by nestin promoter (nestin-GFP), 14 days after inoculation, the tumors were surrounded by the nestin-GFP cells in several cell layers, and 10% (DCX) of the nestin-GFP-positive cells are in the proximity of the tumor (Glass et al., 2005). DCX and nestin are expressed in the ipsilateral SVZ at 7 day after MCAO (Chen et al., 2005). In our experiment, induction of nestin in DCX overexpressing SVZ cells demonstrates that DCX may be involved in the migration of neural precursor SVZ cells toward injured area of brain, such as tumor and stroke.

SVZ cells from rats subjected to MCAO showed up-regulation of DCX expression and increased cell migration. DCX treatment induced cell migration in SVZ and U-87 cells. Knocking down endogenous DCX expression by DCXsiRNA abrogated cell migration in SVZ and U-87 cells. DCX, therefore, directly induces migration of SVZ cells from the adult rat. The SVZ cells contribute to functional recovery after neuronal injury and stroke (Zhang et al., 2001, 2004a,b; Jin et al., 2001). SVZ cells proliferate and migrate to the injured striatum and replace neurons lost after focal ischemia and injury (Zhang et al., 2001, 2004a; Arvidsson et al., 2002; Parent et al., 2002). The majority of the newly generated striatal neurons die, and only ~0.2% of the fraction of striatal neurons after replacement survive (Arvidsson et al., 2002; Parent et al., 2002; Jin et al., 2003; Zhang et al., 2004a). Enhancing the survival of these cells by DCX overexpression, also may benefit restoration of neurological function. Increased DCX expression in tumor cells, may also promote the survival of these cells under potentially lethal insults, such as OGD. Over-expression of DCX in glioma cells may resist toxic agents designed to

destroy them. Thus, the DCX may mediate migration as well as protect these migrating cells during their travels from the site of production in the SVZ to injured tissue. The different microenvironments within the brain, particularly the injured brain, can place migrating neuroblasts at risk (Chen et al., 2005, 2004; Zhang et al., 2004b). Thus, the expression of DCX may ensure the survival of these neural progenitor cells.

Acknowledgments—We thank Dr. Didier Trono for providing us with lentivirus vectors. This work was supported by Stroke Center grant, NINDS# NS23393.

REFERENCES

Amoureux MC, Cunningham BA, Edelman GM, Crossin KL (2000) N-CAM binding inhibits the proliferation of hippocampal progenitor cells and promotes their differentiation to a neuronal phenotype. J Neurosci 20(10):3631–3640.

Arvidsson A, Collin T, Kirik D, Kokaia Z, Lindvall O (2002) Neuronal replacement from endogenous precursors in the adult brain after stroke. Nat Med 8:963–970.

Bai J, Ramos RL, Ackman JB, Thomas AM, Lee RV, LoTurco JJ (2003) RNAi reveals doublecortin is required for radial migration in rat neocortex. Nat Neurosci 6:1277–1283.

Brummelkamp TR, Bernards R, Agami R (2002) A system for stable expression of short interfering RNAs in mammalian cells. Science 296(5567):550–553.

Campisi J (2005a) Suppressing cancer: the importance of being senescent. Science 309(5736):886–887.

Campisi J (2005b) Senescent cells, tumor suppression, and organismal aging: good citizens, bad neighbors. Cell 120(4):513–522.

Carmeliet P, Lampugnani MG, Moons L, Breviario F, Compernolle V, Bono F, Balconi G, Spagnuolo R, Oostuyse B, Dewerchin M, Zanetti A, Angellilo A, Mattot V, Nuyens D, Lutgens E, Carmeliet P, Lampugnani MG, Moons L, Breviario F, Compernolle V, Bono F, Balconi G, Spagnuolo R, Oostuyse B, Dewerchin M, Zanetti A, Angellilo A, Mattot V, Nuyens D, Lutgens E, Clotman F, de Ruiter MC, Gittenberger-de Groot A, Poelmann R, Lupu F, Herbert JM, Collen D, Dejana E (1999) Targeted deficiency or cytosolic truncation of the VE-cadherin gene in mice impairs VEGF-mediated endothelial survival and angiogenesis. Cell 98(2):147–157.

Charalambous C, Hofman FM, Chen TC (2005) Functional and phenotypic differences between glioblastoma multiforme-derived and normal human brain endothelial cells. J Neurosurg 102(4): 699–705.

Chen J, Zacharek A, Zhang C, Jiang H, Li Y, Roberts C, Lu M, Kapke A, Chopp M (2005) Endothelial nitric oxide synthase regulates brain-derived neurotrophic factor expression and neurogenesis after stroke in mice. J Neurosci 25(9):2366–2375.

Chen J, Li Y, Zhang R, Katakowski M, Gautam SC, Xu Y, Lu M, Zhang Z, Chopp M (2004) Combination therapy of stroke in rats with a nitric oxide donor and human bone marrow stromal cells enhances angiogenesis and neurogenesis. Brain Res 1005(1–2):21–28.

Corbo JC, Deuel TA, Long JM, LaPorte P, Tsai E, Wynshaw-Boris A, Walsh CA (2002) Doublecortin is required in mice for lamination of the hippocampus but not the neocortex. J Neurosci 22:7548–7557.

Dimri GP, Lee X, Basile G, Acosta M, Scott G, Roskelley C, Medrano EE, Linskens M, Rubelj I, Pereira-Smith O, Peacocket M, Campisi J (1995) A biomarker that identifies senescent human cells in culture and in aging skin in vivo. Proc Natl Acad Sci U S A 92(20):9363–9367.

Evans RJ, Wyllie FS, Wynford-Thomas D, Kipling D, Jones CJ (2003) A P53-dependent, telomere-independent proliferative life span barrier in human astrocytes consistent with the molecular genetics of glioma development. Cancer Res 63(16):4854–4861.

Feuer R, Pagarigan RR, Harkins S, Liu F, Hunziker IP, Whitton JL (2005) Coxsackievirus targets proliferating neuronal progenitor cells in the neonatal CNS. J Neurosci 25(9):2434–2444.

Francis F, Koulakoff A, Boucher D, Chafey P, Schaar B, Vinet MC, Friocourt G, McDonnell N, Reiner O, Kahn A, McConnell SK, Berwald-Netter Y, Denoulet P, Chelly J (1999) Doublecortin is a developmentally regulated, microtubule-associated protein expressed in migrating and differentiating neurons. Neuron 23:247–256.

Gao X, Bian W, Yang J, Tang K, Kitani H, Atsumi T, Jing N (2001) A role of N-cadherin in neuronal differentiation of embryonic carcinoma P19 cells. Biochem Biophys Res Commun 284(5):1098–1103.

Glass R, Synowitz M, Kronenberg G, Walzlein JH, Markovic DS, Wang LP, Gast D, Kiwit J, Kempermann G, Kettenmann H (2005) Glioblastoma-induced attraction of endogenous neural precursor cells is associated with improved survival. J Neurosci 25(10):2637–2646.

Gleeson JG, Lin PT, Flanagan LA, Walsh CA (1999) Doublecortin is a microtubule-associated protein and is expressed widely by migrating neurons. Neuron 23:257–271.

Hamada-Kanazawa M, Ishikawa K, Nomoto K, Uozumi T, Kawai Y, Narahara M, Miyake M (2004) Sox6 overexpression causes cellular aggregation and the neuronal differentiation of P19 embryonic carcinoma cells in the absence of retinoic acid. FEBS Lett 560(1–3):192–198.

Harada A, Teng J, Takei Y, Oguchi K, Hirokawa N (2002) MAP2 is required for dendrite elongation, PKA anchoring in dendrites, and proper PKA signal transduction. J Cell Biol 158(3):541–549.

Hutter-Paier B, Steiner E, Windisch M (1998) Cerebrolysin protects isolated cortical neurons from neurodegeneration after brief histotoxic hypoxia. J Neural Transm Suppl 53:351–361.

Ikeda T, Xia XY, Xia YX, Ikenoue T (1999) Hyperthermic preconditioning prevents blood-brain barrier disruption produced by hypoxia-ischemia in newborn rat. Brain Res Dev Brain Res 117(1):53–58.

Jin K, Minami M, Lan JQ, Mao XO, Batteur S, Simon RP, Greenberg DA (2001) Neurogenesis in dentate subgranular zone and rostral subventricular zone after focal cerebral ischemia in the rat. Proc Natl Acad Sci U S A 98:4710–4715.

Jin K, Sun Y, Xie L, Peel A, Mao XO, Batteur S, Greenberg DA (2003) Directed migration of neuronal precursors into the ischemic cerebral cortex and striatum. Mol Cell Neurosci 24:171–189.

Krugers HJ, Maslam S, Korf J, Joëls M (2000) The corticosterone synthesis inhibitor prevents metyrapone hypoxia/ischemia-induced loss of synaptic function in the rat hippocampus. Stroke 31:1162.

Kuhn HG, Biebl M, Wilhelm D, Li M, Friedlander RM, Winkler J (2005) Increased generation of granule cells in adult Bcl-2-overexpressing mice: a role for cell death during continued hippocampal neurogenesis. Eur J Neurosci 22(8):1907–1915.

Leventhal C, Rafii S, Rafii D, Shahar A, Goldman SA (1999) Endothelial trophic support of neuronal production and recruitment from the adult mammalian subependyma. Mol Cell Neurosci 13:450–464.

Li G, Satyamoorthy K, Herlyn M (2001) N-cadherin-mediated intercellular interactions promote survival and migration of melanoma cells. Cancer Res 61(9):3819–3825.

Lichtenwalner RJ, Parent JM (2006) Adult neurogenesis and the ischemic forebrain. J Cereb Blood Flow Metab 26(1):1–20.

Linke A, Muller P, Nurzynska D, Casarsa C, Torella D, Nascimbene A, Castaldo C, Cascapera S, Bohm M, Quaini F, Urbanek K, Leri A, Hintze TH, Kajstura J, Anversa P (2005) Stem cells in the dog heart are self-renewing, clonogenic, and multipotent and regenerate infarcted myocardium, improving cardiac function. Proc Natl Acad Sci U S A 102(25):8966–8971.

Livak KJ, Schmittgen TD (2001) Analysis of relative gene expression data using real-time quantitative PCR and the 2(-delta delta C(T)) method. Methods 25(4):402–408.

Lyons SA, Kettenmann H (1998) Oligodendrocytes and microglia are selectively vulnerable to combined hypoxia and hypoglycemia injury in vitro. J Cereb Blood Flow Metab 18:521–530.

Navarro P, Ruco L, Dejana E (1998) Differential localization of VE- and N-cadherins in human endothelial cells: VE-cadherin competes with N-cadherin for junctional localization. J Cell Biol 140(6):1475–1484.

Pardo B, Honegger P (2000) Differentiation of rat striatal embryonic stem cells in vitro: monolayer culture vs. three-dimensional coculture with differentiated brain cells. J Neurosci Res 59(4):504–512.

Parent JM, Vexler ZS, Gong C, Derugin N, Ferriero DM (2002) Rat forebrain neurogenesis and striatal neuron replacement after focal stroke. Ann Neurol 52:802–813.

Reynolds BA, Tetzlaff W, Weiss S (1992) A multipotent EGF-responsive striatal embryonic progenitor cell produces neurons and astrocytes. J Neurosci 11:4565–4574.

Rubinek T, Yu R, Hadani M, Barkai G, Nass D, Melmed S, Shimon I (2003) The cell adhesion molecules N-cadherin and neural cell adhesion molecule regulate human growth hormone: a novel mechanism for regulating pituitary hormone secretion. J Clin Endocrinol Metab 88(8):3724–3730.

Santra M, Skorski T, Calabretta B, Lattime EC, Iozzo RV (1995) De novo decorin gene expression suppresses the malignant phenotype in human colon cancer cells. Proc Natl Acad Sci U S A 92(15):7016–7020.

Santra M, Katakowski M, Zhang RL, Zhang ZG, Meng H, Jiang F, Chopp M (2006) Protection of adult mouse progenitor cells and human glioma cells by de novo decorin expression in an oxygen- and glucose-deprived cell culture model system. J Cereb Blood Flow Metab 2006, in press.

Savarese TM, Jang T, Low HP, Salmonsen R, Litofsky NS, Matuasevic Z, Ross AH, Recht LD (2005) Isolation of immortalized, INK4a/ARF-deficient cells from the subventricular zone after in utero N-ethyl-N-nitrosourea exposure. J Neurosurg 102(1):98–108.

Takei Y, Teng J, Harada A, Hirokawa N (2000) Defects in axonal elongation and neuronal migration in mice with disrupted tau and map1b genes. J Cell Biol 150:989–1000.

Teng J, Takei Y, Harada A, Nakata T, Chen J, Hirokawa N (2001) Synergistic effects of MAP2 and MAP1B knockout in neuronal migration, dendritic outgrowth, and microtubule organization. J Cell Biol 155:65–76.

Wang L, Zhang Z, Wang Y, Zhang R, Chopp M (2004) Treatment of stroke with erythropoietin enhances neurogenesis and angiogenesis and improves neurological function in rats. Stroke 35(7): 1732–1737.

Wiznerowicz M, Trono D (2003) Conditional suppression of cellular genes: lentivirus vector-mediated drug-inducible RNA interference. J Virol 77(16):8957–8961.

Yu X, Shacka JJ, Eells JB, Suarez-Quian C, Przygodzki RM, Beleslin-Cokic B, Lin CS, Nikodem VM, Hempstead B, Flanders KC, Costantini F, Noguchi CT (2002) Erythropoietin receptor signalling is required for normal brain development. Development 129(2): 505–516.

Zhang R, Zhang Z, Wang L, Wang Y, Gousev A, Zhang L, Ho KL, Morshead C, Chopp M (2004a) Activated neural stem cells contribute to stroke-induced neurogenesis and neuroblast migration toward the infarct boundary in adult rats. J Cereb Blood Flow Metab 24:441–448.

Zhang J, Li Y, Chen J, Yang M, Katakowski M, Lu M, Chopp M (2004b) Expression of insulin-like growth factor 1 and receptor in ischemic rats treated with human marrow stromal cells. Brain Res 1030(1):19–27.

Zhang Z, Jiang Q, Jiang F, Ding G, Zhang R, Wang L, Zhang L, Robin AM, Katakowski M, Chopp M (2004c) In vivo magnetic resonance imaging tracks adult neural progenitor cell targeting of brain tumor. Neuroimage 23(1):281–287.

Zhang RL, Zhang ZG, Zhang L, Chopp M (2001) Proliferation and differentiation of progenitor cells in the cortex and the subventricular zone in the adult rat after focal cerebral ischemia. Neuroscience 105:33–41.

Zhang RL, Chopp M, Zhang ZG, Jiang Q, Ewing JR (1997) A rat model of embolic focal cerebral ischemia. Brain Res 766:83–92.

(Accepted 29 June 2006)
(Available online 8 September 2006)